Ab initio study of water dissociation on a charged Pd(111) surface

Karen Fidanyan,[1] Guoyuan Liu,[2] and Mariana Rossi[1, 3]

[1)]*Max Planck Institute for the Structure and Dynamics of Matter, Luruper Chaussee 149, 22761 Hamburg, Germany*

[2)]*Department of Materials Science and Engineering, École Polytechnique Fédérale de Lausanne, CH-1015 Lausanne, Switzerland*

[3)]*Fritz Haber Institute of the Max Planck Society, Faradayweg 4-6, 14195 Berlin, Germany*

(*Electronic mail: mariana.rossi@mpsd.mpg.de)

Interactions between molecules and electrode surfaces play a key role in electrochemical processes and are a subject of extensive research, both experimental and theoretical. In this manuscript, we address the water dissociation reaction on a Pd(111) electrode surface, modelled as a slab embedded in an external electric field. We aim at unraveling the relationship between surface charge and zero-point-energy in aiding or hindering this reaction. We calculate energy barriers with dispersion-corrected density-functional theory and an efficient parallel implementation of the nudged-elastic-band method. We show that the lowest dissociation barrier, and consequently highest reaction rate, takes place when the field reaches a strength that induces a geometric frustration of the water molecule adsorbed on the surface. Zero-point energy contributions to the this reaction, on the other hand, remain nearly constant across a wide range of electric field strengths, despite significant changes in the reactant state.

I. INTRODUCTION

Surface-mediated reactions involving water appear in many technologically relevant processes that lead to hydrogen production or material corrosion[1], for example. In particular in electrocatalysis, a key process to achieve a sustainable economy, the chemistry involved in the water splitting reaction itself can be changed because of the application of a potential bias[2]. In such a system, the structure of water at the interface, the collective properties of the surface, and the electrolyte composition affect the reactions substantially, and present a challenge both for theory and experiments, even when considering idealized electrodes[3–5].

From a theoretical perspective, there are at least three ingredients that must be accounted for when addressing water splitting at (charged) metallic surfaces: charge transfer and reorganization at the interface, (screened) van der Waals interactions between molecules and metal, and the effect of nuclear fluctuations and dynamics on the process of interest. It should be noted that the latter is now accepted to be adequately described only by considering the nuclei as quantum particles[6–11]. While the structure of water at metallic surfaces has been addressed by theoretical models numerous times in the past[12–14], even including potential biases in the simulations[14–17], the surface-mediated dissociation of water has received comparatively less attention from theoretical work. Several groups reported studies of the splitting of water molecules on various transition metals[18–24], but to the best of our knowledge, never accounting at the same time for potential biases, long-range dispersion interactions and nuclear quantum effects (NQE).

Specifically, accounting for a potential bias in first-principles simulation is not trivial. A number of methods to include a potential bias in the slab model were proposed, including various degrees of approximation,[25–32] without the adoption of a common "default" approach. A fully *ab initio* approach based on the non-equilibrium Green's function formalism[33] presents a very high computational hurdle

for the simulation of rare reactive events. Other recent approaches like potentiostats that can be coupled to *ab initio* simulations[30], or grand-canonical self-consistent field (SCF) techniques[29] could provide a good compromise between efficiency and accuracy, but still present an elevated computational cost. Effecitve 2D-periodic models like the effective screening medium (ESM)[25] have allowed the simulation of *ab initio* molecular dynamics of water at charged metal interfaces[17,34] more than 15 years ago. With the ESM, the water dissociation on a platinum surface under potential bias could be studied by *ab initio* molecular dynamics (AIMD)[24,35], which presents a remarkable achievement. However, only relatively short molecular dynamics (MD) trajectories (of a few picoseconds) could be simulated, which considerably limits the predictive power of such simulations given that the reaction is a rare event in this timescale. Interestingly, it has been recently shown from classical MD simulations, that results obtained by simulations with a constant applied potential between two electrodes in a 2D-periodic model were indistinguishable from those obtained from a 3D-periodic model with a large metallic slab in the center of the simulation cell, and an applied electric field[36] – a possibility that can also simplify *ab initio* simulations of electrochemical interfaces.

In this paper, we employ an applied electric-field setup to address the water dissociation reaction directly, and understand the role of different surface charges and nuclear quantum effects in modifying the reaction dynamics. We study a model system of a water monomer adsorbed on a Pd(111) surface, modelled by density-functional theory. Different charges on the surface of the metal are realized by the application of an electric field on a thick Pd(111) slab, which mimics a potential bias. We report the changes in reaction barriers and rates and the effects of zero-point energy at different field strengths. These results serve as ground-work for more complex system setups and simulation protocols. They also give valuable insights on how far NQE and electric fields can impact this reaction.

II. METHODS

We simulated a Pd(111) surface by a slab of 7 atomic layers in a periodic cell including a large vacuum layer of 64 Å, using the FHI-aims code[38]. A dipole correction[39] was applied to compensate for spurious interactions between periodic images. We employed the PBE exchange-correlation functional[40] augmented by dispersion interactions as described by the screened vdW$^{\text{surf}}$ model[41], with the coefficients for Pd taken from Ref.[42]. *Light* default settings of FHI-aims were used for basis sets, and modified *light* settings with double radial density were used for numerical real-space grids. The lateral dimensions of the Pd slab were chosen as 4×4 unit cells, simulated with a 3×3 k-points mesh. We placed the metallic slab at the center of the unit cell.
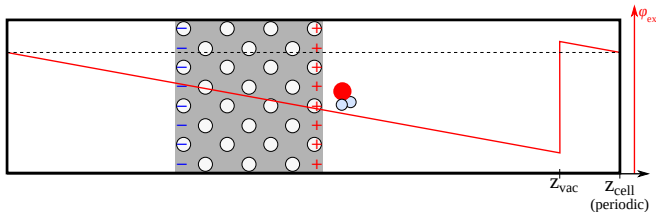

FIG. 1. Schematic of simulation setup. A periodic cell is permeated by an external electrostatic potential φ_{ext} with a discontinuity in vacuum far away from the slab.

The potential bias is mimicked by an external electric field permeating the system, which is implemented as a saw-tooth potential with the potential step in the vacuum region (see Fig.1). The polarization induced by the electric field causes the surfaces of the slab to effectively become capacitor plates with opposite charges. We assured that the slab is thick enough to screen the surfaces from each other, by analyzing the charge density distribution at self consistency, under different field strengths. Of course, the surfaces remain coupled by the charge conservation constraint. We observed a linear dependence of the surface charge on the applied electric field in a range from –10 to +10 V/Å. An increase of the field by 1 V/Å induced a surface charge of 0.0364 electron per Pd atom, which is equivalent to 8.734 C/cm^2. The surfaces at zero electric field are slightly negatively charged, which offsets the linear dependence by –0.012 e per atom. We will call a field "negative" or "positive" according on the charge that it induces to the surface of interest.

For the phonon calculations, a modified version[43] of the Phonopy package[44] was used, and either only the water molecule, or the molecule and the first layer of the surface were included to build the Hessian. The deeper layers of the surface were included as a rigid environment. By doing so, we lose the coupling Hessian elements between the atoms of the molecule and the surface beyond the first layer, which can affect low-frequency molecule-surface phonons. Since the molecule is small and light, we assume that long-wave collective vibrations of a surface do not play a significant role in water reactions, because the chemically relevant frequencies

of the H-O-H bending and O-H stretching are not substantially affected.

The reaction paths were obtained using the climbing-image nudged elastic band (CI-NEB) method[45]. We used a new implementation of CI-NEB in the i-PI[46] code, in which several instances of the FHI-aims code could connect simultaneously to i-PI and efficiently calculate the forces on each replica in parallel. This implementation is described in detail in Ref.[47] and is available through the main repository of the code. We used a NEB path with 9 intermediate replicas with the spring strength of 20-40 eV/Å. We used the FIRE[48] algorithm for the optimization. The tolerance for forces was set to 0.05 eV/Å for the optimisation of the NEB path and to 0.01 eV/Å for the climbing-image optimisation.

III. ADSORPTION OF WATER ON A CHARGED PD(111) SURFACE

We have found the preferred adsorption geometries of a single water molecule at Pd(111) surface for different electric field strengths and report them in Fig. 2.
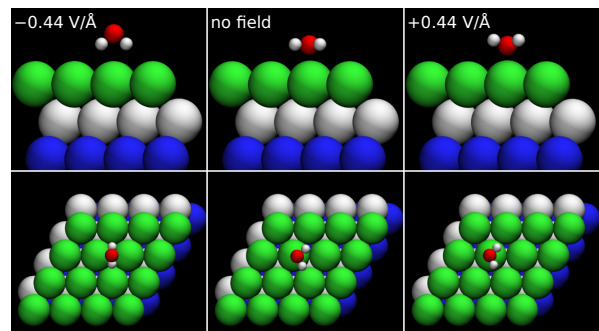

FIG. 2. Adsorption geometries of a single water molecule on the Pd(111) surface under –0.44 V/Å (left), no field (center) and +0.44 V/Å (right). Large green, white and blue spheres denote the 1st, 2nd and 3rd layers of the Pd(111) surface, respectively.

We found that the water molecule prefers a flat orientation if no field is applied, which agrees with previous works[18–20]. In a negative electric field, the flat orientation remains up to –0.37 V/Å, after which the molecule "stands up" pointing both hydrogen atoms towards the surface. In a positive field, the molecule deviates gradually from the flat geometry, and hydrogen atoms turn more and more towards the vacuum. These observations are also in qualitative agreement with earlier work, for example regarding a water monomer on Au(111) treated with non-equilibrium Green's functions[33]. We did not observe any abrupt changes in the range between –0.37 and +1 V/Å.

We calculated the adsorption energies of water E_{ads} in the presence of an electric field. The references to calculate E_{ads} at each field strength were taken as the isolated subsystems optimized in the presence of the respective electric field embedding. The adsorption energies are summarized in Fig. 3a and Table I. The highest adsorption energy is observed when

TABLE I. Adsorption energy E_{ads}, potential energy barrier E_a, ZPE-corrected barrier of dissociation and corresponding quasi-harmonic quantum TST dissociation rates k_d of a water monomer on a Pd(111) surface, depending on the applied electric field. The electric field of 1 V/Å corresponds to the surface charge of 0.0364 electron per Pd atom (8.734 C/cm^2). The values are calculated with PBE + vdW^{surf}, unless specified otherwise.

Electric field (V/Å)	E_{ads} (eV)	E_a (eV)	ZPE-corrected E_a (eV)	$k_d^{300\,K}$ (s^{-1})	Note
+0.74	0.40	1.32	1.12	4.3×10^{-5}	
+0.44	0.44	1.18	0.98	8.6×10^{-3}	
+0.15	0.47	1.08	0.86	5.3×10^{-1}	
+0.07	0.48	1.06	—	—	
no field	0.48	1.03	0.83	4.7	this work
	0.31	—	—	—	this work, no vdW
	0.33	—	—	—	[37] PW91, no vdW
	—	1.12	—	—	[18] PBE, no vdW
	0.22	1.09	0.87	—	[19] PW91, no vdW
	0.30	1.05	—	—	[20] PW91, no vdW
	0.31	1.15	0.96	—	[21] PW91, no vdW
−0.07	0.45	1.02	—	—	
−0.15	0.41	1.00	0.80	$1.4 \times 10^{+1}$	
−0.29	0.34	0.98	0.78	$1.9 \times 10^{+1}$	
−0.44	0.31	1.02	0.85	2.4×10^{-1}	
−0.74	0.30	1.01	0.90	1.1×10^{-1}	
−1.00	0.30	—	—	—	

no electric field or a slight positive field of 0.07 V/Å is applied. The value obtained without an electric field is 0.48 eV, which is larger than the values of 0.22-0.31 eV reported in previous studies[19–21], and with which we will compare below. The reason for this discrepancy is that no van der Waals (vdW) interactions were included in these previous studies, as we show in Table I. When increasing the field towards positive values, E_{ads} gradually decreases (i.e., the adsorbed system becomes less stable). When a negative field is applied, E_{ads} also gradually decreases down to a field of –0.44 V/Å, after which it remains approximately constant. This change of the trend corresponds to the flip of the preferred adsorption orientation discussed above.

We investigated how the character of the bond between the molecule and the surface changes with an electric field by projecting the total electronic DOS on the atoms. We show such projected DOS in Fig. 4. By comparing the positions of the molecular orbitals in the gas-phase to those on the surface, we observe in Fig. 4 that what used to be the HOMO level of the water molecule in isolation becomes substantially broader for field values ranging from +0.74 to –0.15 V/Å, which points toward a hybridization with the Pd d-bands. For more negative fields, the hybridization is drastically reduced, which is consistent with the "standing" orientation of the water molecule and the character of the HOMO level of water (centered on oxygen). This is also reflected on the Hirshfeld and Mulliken analysis of the charge accummulated on the molecule, shown in Fig. 3b. On a positively charged surface, Hirshfeld and Mulliken analysis agree for the total charge, even if they predict different values for the individual atoms. The molecule donates roughly 0.2 e to the surface, indicating orbital hybridization and electron transfer from the molecule to the surface. At an electric field below –0.44 V/Å, when the molecule "stands", the Mulliken analysis shows, in contrast, a negli-

gibly small charge, while the Hirshfeld method shows about –0.15 e. We interpret the discrepancy between the Hirshfeld and Mulliken charges as a specific feature of the Hirshfeld definition of charge, which assigns local changes of the electron density to atoms proportionally to their free-atom electron density at the considered point. Therefore, a change of the "tail" of surface density can be assigned to the molecule even if there is no hybridization of the orbitals of the surface and the molecule.

IV. REACTION PATHS IN AN ELECTRIC FIELD

The nudged elastic band (NEB) paths and corresponding energies of the nodes for the zero-field case are shown in figure 5. Representative paths for positive and negative electric fields are given in the Supplemental Information. We verified the transition states by a normal mode analysis. In all cases, the transition state has exactly one imaginary-frequency mode, which corresponds to a direction of barrier crossing. The geometry of the transition state has little dependence on the surface charge, especially if compared to the reactant state. The activation energy E_a for each bias is summarized in Fig. 6 and in Table I.

For zero bias, our E_a value lies below (by 20-120 meV) previously reported calculations[18–21], which also did not include dispersion interactions. Many previous work employed the PW91 exchange-correlation (XC) potential, but it was shown on various metals that the water dissociation barrier calculated by PW91 and PBE are almost identical, e.g. see the SI of Ref.[21]. Thus, the discrepancy with literature is consistent with the observation of Litman et $al.$ that inclusion of vdW interactions decreases the barrier of dissociation of water on metals[23]. The lowest barrier is observed at –0.29 V/Å, directly
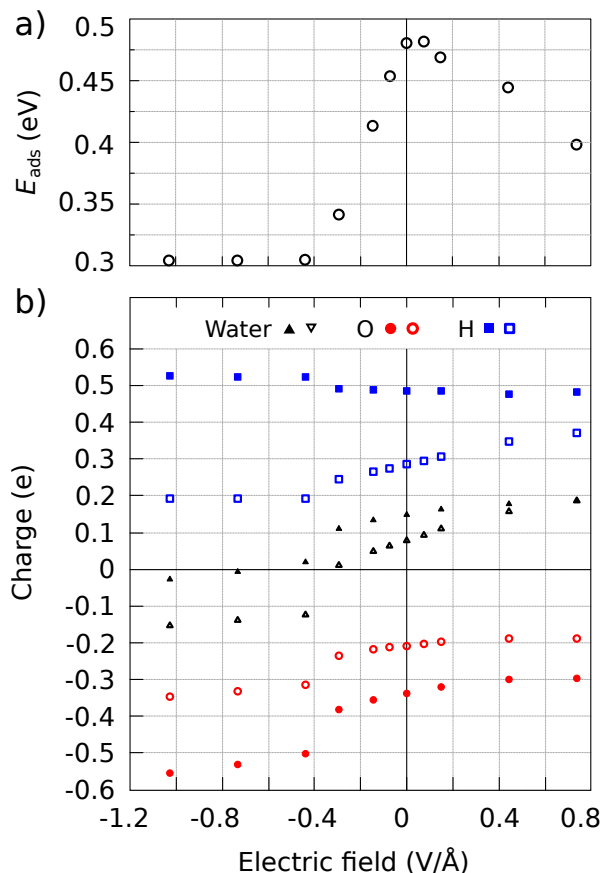
FIG. 3. a) Adsorption energy of a single water molecule on the Pd(111) surface as a function of the applied electric field. The values are calculated with PBE + vdW^{surf}. b) Charge induced on the adsorbed water molecule depending on the applied electric field, measured by the Mulliken (filled points) and Hirshfeld (empty points) analysis. The black triangles show the total charge on the molecule, and the blue squares (red circles) show H (O) contributions to it.
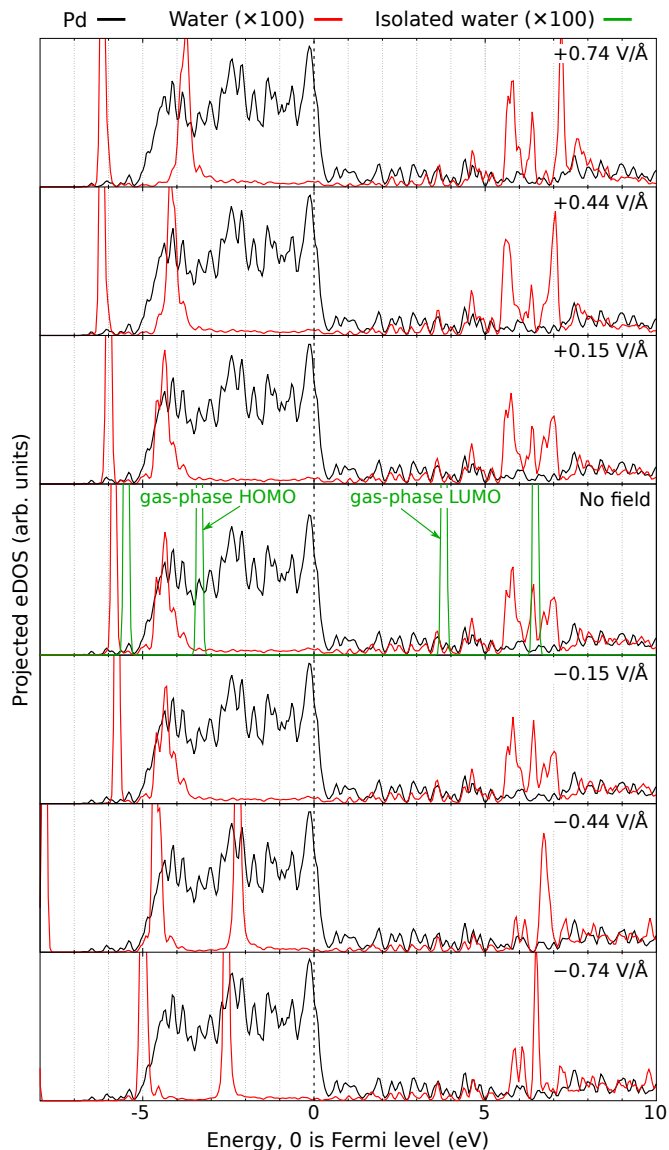

FIG. 4. Electronic density of states projected on the atomic species at different values of an external electric field. The red lines denote Pd and the black lines the sum of O and H contributions. Green curves on the zero-field plot show the DOS of an isolated water molecule, aligned so that the 1s orbital of its oxygen matches that of the full system.

before the water molecule changes its adsorption orientation. Positive electric fields only increase E_a. Analysing the MEP, we speculate that the reason for this behavior is that positive field strengths stabilize the O-Pd bond at the reactant, as evidenced by the charge-transfer behaviour. This strengthening makes it harder for water to move towards the point where the TS is. Negative field strengths destabilize the bond, matching, in fact, the strength of the O-Pd bond at around the flipping point. Beyond the flipping point, the molecule is physisorbed, but has to flip back in order to reach the transition state (see MEPs in SI), which again costs energy.

As discussed previously in the literature, the main nuclear quantum effect that affects water dissociation on metallic surfaces is zero-point-energy, with tunneling playing an insignificant role at most relevant temperatures (e.g. around room temperature)[23]. We confirm this observation here by an analysis of the frequency of the TS mode at all electric field strengths, reported in the SI. We estimate tunneling crossover temperatures to be below 30 K for all field strengths. We thus calculated the harmonic ZPE contributions to reactant and tran-

sition state, and summarize the changes of the dissociation barrier in Fig. 6 and in Table I. We note that a low-frequency vibrational mode of the reactant, corresponding to the rotation of water hydrogens around the oxygen, parallel to the surface plane, becomes progressively lower in frequency and even slightly negative (-5 cm^{-1}) towards higher positive field values. We have tightened optimization thresholds and increased numerical and basis set accuracies to confirm this observation. First, we can conclude that this model system is indeed slightly unstable above +0.44 V/Å within the harmonic approximation, and the molecule could be freely rotating paral-
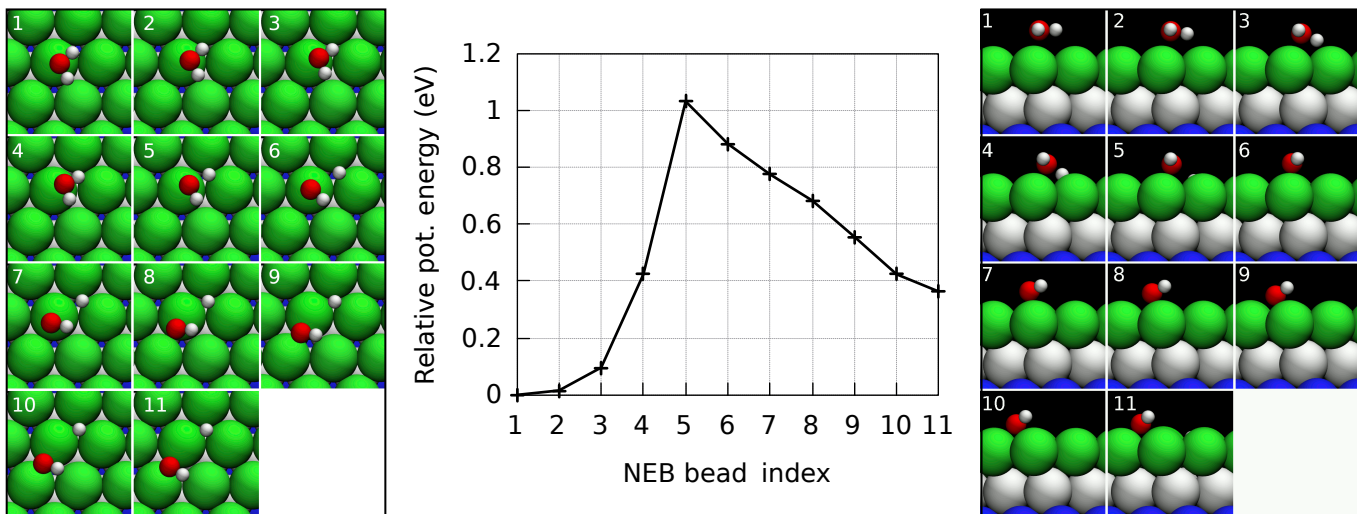
FIG. 5. Potential energy along the MEP with no field applied, found by the CI-NEB algorithm, with the reactant state indexed as 1. Individual NEB node geometries of the reaction path are shown and labeled from top and side perspectives. Node 5 is the transition state. Large green, white and blue spheres denote the 1st, 2nd and 3rd layers of the Pd(111) surface, respectively.
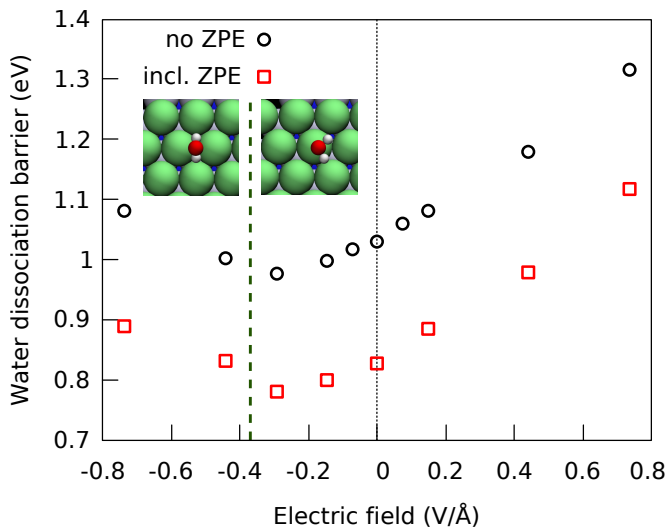

FIG. 6. The energy barrier of water splitting calculated by CI-NEB algorithm. Black circles show the potential energy barrier, and red squares show the ZPE-corrected barrier, calculated in the harmonic approximation. The dashed green line marks the border between two orientations of the reactant state.

lel to the surface plane, which could lead to an entropic stabilization at finite temperatures. Second, these modes do not play a significant role on the water dissociation path and, because this is a feature of the model that would disappear if water was embedded in an H-bonded network, for the ZPE analysis we consistently ignored this mode in all calculations. We should add that because the mode is so low in energy (always below 30 cm^{-1}), its contribution would always be less than 6 meV to the total ZPE.

The ZPE contribution decreases the barrier by roughly 0.19-0.20 eV at all points except –0.44 V/Å, where the de-

crease is 0.17 eV. This is a considerable contribution in this case, representing $\approx$ 20% of the barrier height. However, such a constant effect is somewhat surprising, given that the geometry of the reactant state changes considerably. In order to resolve the effects of ZPE, we analyzed the vibrational density of states (vDOS) spectra of the reactant and transition states, which are shown in Fig. 7, top and bottom, respectively. The most pronounced difference appears in the two hindered rotation modes of the reactant, which shift sharply from the range of 400-500 cm^{-1} down to 200-320 cm^{-1} when the field reaches –0.44 V/Å (the flipping point). These modes are shown in Fig. 8. It is important to note that hindered rotation modes are expected to be strongly anharmonic and thermally populated, as quantified in Ref.[49], therefore the harmonic analysis presented here gives only an estimate of the effect.

Despite multiple shifts in the low-frequency part of the spectrum, the ZPE is dominated by the high-frequency modes, namely the H-O-H bending mode and one of the two O-H stretching modes, which exist in the reactant state and disappear at the transition state. This is the main source of difference between the reactant and transition state contributions. We present a detailed analysis of the impact of particular modes on the total ZPE in the SI. Even though these modes also present a strong variation in the reactant state under different applied electric fields, the ZPE contributions are compensated between product and reactant states, as an analysis of the cumulative ZPE contribution shows (see SI), resulting in the essentially constant ZPE correction to the reaction barrier.

In order to estimate how much the reaction rates can be changed due to the electric field effect, we report reaction rates as calculated from the quantum quasi-harmonic approximation (Eq. 13 in Ref.[23]). We report these rates at a temperature of 300 K in Table I. This is an artificial temperature because the single molecule would have a considerable desorption probability at this temperature and would surely be very
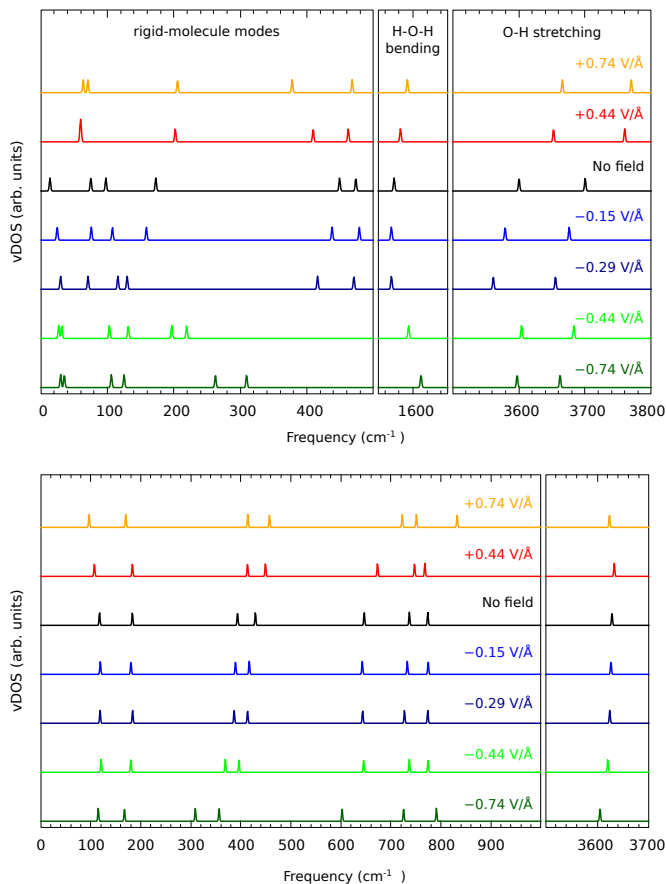
FIG. 7. Vibrational density of states of the reactant state (top) and of the transition state (bottom) of the water splitting reaction on a Pd(111) surface at different electric field values. The lowest-frequency mode of the reactant state becomes unstable at +0.44 and +0.74 V/Å, therefore it is not shown.

FIG. 8. Hindered rotation modes of a water molecule on a Pd(111) surface at –0.15 V/Å (top) and –0.44 V/Å (bottom).

V. CONCLUSIONS

We presented an *ab initio* study of water dissociation on the Pd(111) surface using a slab model embedded in an electric field in a 3D periodic setup. The electric field effectively induces opposite charges on each surface of the thick metallic slab, and mimics the effect of an applied potential bias at the metallic electrode surface.

Analysing the reaction paths at different field strengths, we concluded that the main feature that affects the reaction barrier is the geometry of the reactant state, which is strongly influenced by the applied field. Between field strengths of –0.3 and –0.4 V/Å, the reactant state abruptly changes its geometry, with the water molecule pointing the hydrogen atoms to the surface. We demonstrated that the lowest barrier (and consequently highest reaction rate) for the monomer dissociation lies at the electric field strength at which the molecule has these two adsorption geometries equally preferred, i.e., at the flipping point. We rationalized that at this point, the water-surface bond is optimally weakened, making it easier for the system to reach its transition state. We evaluated NQE limited to ZPE in the harmonic approximation and demonstrated that it reduces the barrier by roughly 0.2 eV at all field strengths. The reason for such a weak dependence on the field strength is the dominant role of bond stretching modes on the ZPE of the reaction and the mutual cancellation of contributions of different vibrational modes between reactant and transition states.

Although we studied a highly idealized system, we expect these findings to be relevant for more complex scenarios. Chemistry under applied electric fields is a booming field in its own right, and extending some of the protocols presented in this paper for methods that can capture nuclear tunneling could open exciting new avenues for situations where such effects play a role[50]. In electrochemistry, the change in orientation of the first water layer under different potential biases has been observed experimentally[5] and the role of these effects in the chemistry that happens at these interfaces is still not fully understood. The observation that the water splitting reaction at a single-molecule level is optimally enhanced right around the flipping point should also be of interest in

mobile. However, a single adsorbed water molecule is already a model system in this context. Therefore, these numbers serve only to build a more quantitative intuition. As expected, the suppression of the reaction rate at positive field values (up to 5 orders of magnitude) is much more significant than its increase at negative field values (only up to a factor of 4). We predict that the flipping point of the first water layer will also limit the increase of this reaction rate when water is at the liquid state. Because in the liquid, for the first water layer to flip, hydrogen bonds would need to be broken, the flipping point should happen at considerably larger field strengths. Taking the H-bond strength to be between 40-60 meV in the liquid, each water having four H-bonds to break, and that from our calculations we need about 0.5 V/Å to change the energy of water by 0.24 eV, the field strength for the flipping point in the liquid should be around 0.9 V/Å.

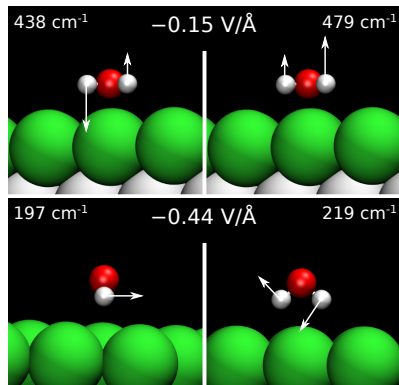these situations. Moreover, the observation that the ZPE contributions are almost constant throughout a large variety of field strengths could simplify more involved simulation protocols involving MD simulations, where one perhaps could estimate NQE corrections or changes at a single field strength and propagate that to others – even if with care, because the effect of NQE may not be uniform across field strengths for other liquid water properties[51]. Finally, we note that we constrained the total charge of the simulation cell to be zero, while a real electrode would allow charge fluctuations on a larger scale and, possibly, with a lower energy penalty – a possibility that should be explored in future work.

DATA AVAILABILITY STATEMENT

Phonon calculations for the initial and transition states of the water splitting reaction, and the geometry relaxations of the adsorbed reactants and products for different values of an electric field are uploaded to the NOMAD repository. The dataset DOI is 10.17172/NOMAD/2022.09.15-1.

[1] T. Würger, C. Feiler, G. B. Vonbun-Feldbauer, M. L. Zheludkevich, and R. H. Meißner, "A first-principles analysis of the charge transfer in magnesium corrosion," Scientific Reports **10**, 15006 (2020).

[2] H. N. Nong, L. J. Falling, A. Bergmann, M. Klingenhof, H. P. Tran, C. Spöri, R. Mom, J. Timoshenko, G. Zichittella, A. Knop-Gericke, S. Piccinin, J. Pérez-Ramírez, B. R. Cuenya, R. Schlögl, P. Strasser, D. Teschner, and T. E. Jones, "Key role of chemistry versus bias in electrocatalytic oxygen evolution," Nature **587**, 408–413 (2020).

[3] Y.-H. Wang, S. Zheng, W.-M. Yang, R.-Y. Zhou, Q.-F. He, P. Radjenovic, J.-C. Dong, S. Li, J. Zheng, Z.-L. Yang, G. Attard, F. Pan, Z.-Q. Tian, and J.-F. Li, "In situ Raman spectroscopy reveals the structure and dissociation of interfacial water," Nature **600**, 81–85 (2021).

[4] Y. Tong, F. Lapointe, M. Thämer, M. Wolf, and R. K. Campen, "Hydrophobic water probed experimentally at the gold electrode/aqueous interface," Angewandte Chemie International Edition **56**, 4211–4214 (2017).

[5] M. F. Toney, J. N. Howard, J. Richer, G. L. Borges, J. G. Gordon, O. R. Melroy, D. G. Wiesler, D. Yee, and L. B. Sorensen, "Voltage-dependent ordering of water molecules at an electrode–electrolyte interface," Nature **368**, 444–446 (1994).

[6] K. Laasonen, M. Sprik, M. Parrinello, and R. Car, ""Ab initio" liquid water," The Journal of chemical physics **99**, 9080–9089 (1993).

[7] D. Marx, M. E. Tuckerman, J. Hutter, and M. Parrinello, "The nature of the hydrated excess proton in water," Nature **397**, 601–604 (1999).

[8] D. Marx, M. E. Tuckerman, and M. Parrinello, "Solvated excess protons in water: quantum effects on the hydration structure," Journal of Physics: Condensed Matter **12**, A153–A159 (2000).

[9] X.-Z. Li, M. I. J. Probert, A. Alavi, and A. Michaelides, "Quantum Nature of the Proton in Water-Hydroxyl Overlayers on Metal Surfaces," Physical Review Letters **104**, 066102 (2010).

[10] M. Rossi, H. Liu, F. Paesani, J. Bowman, and M. Ceriotti, "Communication: On the consistency of approximate quantum dynamics simulation methods for vibrational spectra in the condensed phase," The Journal of Chemical Physics **141**, 181101 (2014).

[11] M. Ceriotti, W. Fang, P. G. Kusalik, R. H. McKenzie, A. Michaelides, M. A. Morales, and T. E. Markland, "Nuclear quantum effects in water and aqueous systems: Experiment, theory, and current challenges," Chemical Reviews **116**, 7529–7550 (2016), pMID: 27049513.

[12] J. Carrasco, J. Klimeš, and A. Michaelides, "The role of van der Waals forces in water adsorption on metals," The Journal of Chemical Physics **138**, 024708 (2013).

[13] S. Izvekov and G. A. Voth, "Ab initio molecular dynamics simulation of the Ag(111)-water interface," The Journal of Chemical Physics **115**, 7196–7206 (2001).

[14] A. Groß and S. Sakong, "Ab initio simulations of water/metal interfaces," Chemical Reviews **122**, 10746–10776 (2022).

[15] L. S. Pedroza, A. Poissier, and M.-V. Fernández-Serra, "Local order of liquid water at metallic electrode surfaces," The Journal of Chemical Physics **142**, 034706 (2015).

[16] Z. K. Goldsmith, M. F. C. Andrade, and A. Selloni, "Effects of applied voltage on water at a gold electrode interface from ab initio molecular dynamics," Chemical Science **12**, 5865–5873 (2021).

[17] O. Sugino, I. Hamada, M. Otani, Y. Morikawa, T. Ikeshoji, and Y. Okamoto, "First-principles molecular dynamics simulation of biased electrode/solution interface," Surface Science **601**, 5237–5240 (2007).

[18] G.-C. Wang, S.-X. Tao, and X.-H. Bu, "A systematic theoretical study of water dissociation on clean and oxygen-preadsorbed transition metals," Journal of Catalysis **244**, 10–16 (2006).

[19] Y. Cao and Z.-X. Chen, "Theoretical studies on the adsorption and decomposition of H2O on Pd(111) surface," Surface Science **600**, 4572–4583 (2006).

[20] A. A. Phatak, W. N. Delgass, F. H. Ribeiro, and W. F. Schneider, "Density functional theory comparison of water dissociation steps on Cu, Au, Ni, Pd, and Pt," The Journal of Physical chemistry c **113**, 7269–7276 (2009).

[21] J. L. C. Fajín, M. N. D. S. Cordeiro, F. Illas, and J. R. B. Gomes, "Descriptors controlling the catalytic activity of metallic surfaces toward water splitting," Journal of Catalysis **276**, 92–100 (2010).

[22] D. Donadio, L. M. Ghiringhelli, and L. D. Site, "Autocatalytic and Cooperatively Stabilized Dissociation of Water on a Stepped Platinum Surface," Journal of the American Chemical Society **134**, 19217 – 19222 (2012).

[23] Y. Litman, D. Donadio, M. Ceriotti, and M. Rossi, "Decisive role of nuclear quantum effects on surface mediated water dissociation at finite temperature," The Journal of Chemical Physics **148**, 102320 (2018).

[24] Y. Qian, I. Hamada, M. Otani, and T. Ikeshoji, "Inhibition of water dissociation on a pitted Pt(111) surface: First principles study," Catalysis Today **202**, 163–167 (2013), electrocatalysis.

[25] M. Otani and O. Sugino, "First-principles calculations of charged surfaces and interfaces: A plane-wave nonrepeated slab approach," Phys. Rev. B **73**, 115407 (2006).

[26] N. Bonnet, T. Morishita, O. Sugino, and M. Otani, "First-principles molecular dynamics at a constant electrode potential," Phys. Rev. Lett. **109**, 266101 (2012).

[27] R. Sundararaman, W. A. Goddard, and T. A. Arias, "Grand canonical electronic density-functional theory: Algorithms and applications to electrochemistry," The Journal of Chemical Physics **146**, 114104 (2017).

[28] S. Surendralal, M. Todorova, M. W. Finnis, and J. Neugebauer, "First-principles approach to model electrochemical reactions: Understanding the fundamental mechanisms behind Mg corrosion," Phys. Rev. Lett. **120**, 246801 (2018).

[29] S. Hagiwara, C. Hu, S. Nishihara, and M. Otani, "Bias-dependent diffusion of a H2O molecule on metal surfaces by the first-principles method under the grand-canonical ensemble," Phys. Rev. Materials **5**, 065001 (2021).

[30] F. Deißenbeck, C. Freysoldt, M. Todorova, J. Neugebauer, and S. Wippermann, "Dielectric properties of nanoconfined water: A canonical thermopotentiostat approach," Phys. Rev. Lett. **126**, 136803 (2021).

[31] R. Khatib, A. Kumar, S. Sanvito, M. Sulpizi, and C. S. Cucinotta, "The nanoscale structure of the Pt-water double layer under bias revealed," Electrochimica Acta **391**, 138875 (2021).

[32] L. J. V. Ahrens-Iwers, M. Janssen, S. R. Tee, and R. H. Meiß ner, "ELECTRODE: An electrochemistry package for atomistic simulations," The Journal of Chemical Physics **157**, 084801 (2022), 2203.15461.

[33] L. S. Pedroza, P. Brandimarte, A. R. Rocha, and M.-V. Fernández-Serra, "Bias-dependent local structure of water molecules at a metallic interface," Chem. Sci. **9**, 62–69 (2018).

[34] M. Otani, I. Hamada, O. Sugino, Y. Morikawa, Y. Okamoto, and T. Ikeshoji, "Structure of the water/platinum interface – a first principles simulation under bias potential," Physical Chemistry Chemical Physics **10**, 3609–3612 (2008).

[35] T. Ikeshoji, M. Otani, I. Hamada, and Y. Okamoto, "Reversible redox reaction and water configuration on a positively charged platinum surface: first principles molecular dynamics simulation," Phys. Chem. Chem. Phys. **13**, 20223–20227 (2011).

[36] T. Dufils, G. Jeanmairet, B. Rotenberg, M. Sprik, and M. Salanne, "Simulating electrochemical systems by combining the finite field method with a constant potential electrode," Phys. Rev. Lett. **123**, 195501 (2019).

[37] A. Michaelides, V. A. Ranea, P. L. de Andres, and D. A. King, "General model for water monomer adsorption on close-packed transition and noble metal surfaces," Phys. Rev. Lett. **90**, 216102 (2003).

[38] V. Blum, R. Gehrke, F. Hanke, P. Havu, V. Havu, X. Ren, K. Reuter, and M. Scheffler, "Ab initio molecular simulations with numeric atom-centered orbitals," Computer Physics Communications **180**, 2175 – 2196 (2009).

[39] J. Neugebauer and M. Scheffler, "Adsorbate-substrate and adsorbate-adsorbate interactions of Na and K adlayers on Al(111)," Phys. Rev. B **46**, 16067–16080 (1992).

[40] J. P. Perdew, K. Burke, and M. Ernzerhof, "Generalized gradient approximation made simple," Phys. Rev. Lett. **77**, 3865–3868 (1996).

[41] V. G. Ruiz, W. Liu, E. Zojer, M. Scheffler, and A. Tkatchenko, "Density-functional theory with screened van der Waals interactions for the modeling of hybrid inorganic-organic systems," Phys. Rev. Lett. **108**, 146103 (2012).

[42] V. G. Ruiz, W. Liu, and A. Tkatchenko, "Density-functional theory with screened van der Waals interactions applied to atomic and molecular adsorbates on close-packed and non-close-packed surfaces," Phys. Rev. B **93**, 035118 (2016).

[43] K. Fidanyan, "Modified Phonopy-FHI-aims interface," `https://github.com/fidanyan/phonopy` (2019), accessed: 2022-12-06.

[44] A. Togo and I. Tanaka, "First principles phonon calculations in materials science," Scr. Mater. **108**, 1–5 (2015).

[45] G. Henkelman, B. P. Uberuaga, and H. Jónsson, "A climbing image nudged elastic band method for finding saddle points and minimum energy paths," The Journal of chemical physics **113**, 9901–9904 (2000).

[46] V. Kapil, M. Rossi, O. Marsalek, R. Petraglia, Y. Litman, T. Spura, B. Cheng, A. Cuzzocrea, R. H. Meißner, D. M. Wilkins, B. A. Helfrecht, P. Juda, S. P. Bienvenue, W. Fang, J. Kessler, I. Poltavsky, S. Vandenbrande, J. Wieme, C. Corminboeuf, T. D. Kühne, D. E. Manolopoulos, T. E. Markland, J. O. Richardson, A. Tkatchenko, G. A. Tribello, V. V. Speybroeck, and M. Ceriotti, "i-PI 2.0: A universal force engine for advanced molecular simulations," Computer Physics Communications **236**, 214 – 223 (2019).

[47] K. Fidanyan, *Theoretical investigations of nuclear quantum effects in weakly bonded metal-molecular interfaces*, Ph.D. thesis, Humboldt-Universität zu Berlin (2022).

[48] E. Bitzek, P. Koskinen, F. Gähler, M. Moseler, and P. Gumbsch, "Structural Relaxation Made Simple," Physical Review Letters **97**, 170201 (2006).

[49] M. Rossi, "Progress and challenges in ab initio simulations of quantum nuclei in weakly bonded systems," The Journal of Chemical Physics **154**, 170902 (2021), 2103.04206.

[50] O. Kirshenboim, A. Frenklah, and S. Kozuch, "Switch chemistry at cryogenic conditions: quantum tunnelling under electric fields," Chemical Science **12**, 3179–3187 (2020).

[51] G. Cassone, J. Sponer, and F. Saija, "Ab Initio Molecular Dynamics Studies of the Electric-Field-Induced Catalytic Effects on Liquids," Topics in Catalysis **65**, 40–58 (2022).

Supplementary material: Ab initio study of water dissociation on a charged Pd(111) surface

Karen Fidanyan and Mariana Rossi[*]

Max Planck Institute for the Structure and Dynamics of Matter,

Luruper Chaussee 149, 22761 Hamburg, Germany

Guoyuan Liu

Department of Materials Science and Engineering,

École Polytechnique Fédérale de Lausanne, CH-1015 Lausanne, Switzerland

I. WATER DISSOCIATION PATHS WITH NON-ZERO ELECTRIC FIELDS

Dissociation paths for –0.74 and +0.74 V/Å and the corresponding energies are shown in figure S1. Despite different reactant geometries, the transition states of the reaction are quite similar.

II. MODE-RESOLVED ZPE EFFECT ON THE DISSOCIATION BARRIER

We show the contributions to the ZPE from individual vibrational modes of the adsorbed water molecule in table S1.

In order to see more clearly how the shifts of the vibrational modes contribute to the total zero point energy (ZPE) effect on the reaction barrier, we calculate a cumulative ZPE difference between the reactant and the transition state as follows:

$$\Delta_{\text{cumul}}^{\text{ZPE}}(\omega) = \sum_{\omega_i \leq \omega} \frac{\hbar \omega_i^{\text{TS}}}{2} - \sum_{\omega_i \leq \omega} \frac{\hbar \omega_i^{\text{ini}}}{2}, \tag{1}$$

where ω_i^{TS} and ω_i^{ini} are the normal modes of the transition state and the reactant, respectively. We show $\Delta_{\text{cumul}}^{\text{ZPE}}(\omega)$ in figure S2.

One can see that despite multiple shifts of the individual modes, all the ZPE differences between the most distant electric field values of + and –0.74 V/Å below 1000 cm^{-1} cancel out, ending up with almost equal ZPE contribution to the barrier.

---

[*] mariana.rossi@mpsd.mpg.de

TABLE S1. The frequencies of the individual vibrational modes of the water molecule adsorbed at Pd(111) surface ("ini") and of the transition state of its dissociation ("TS"). The values are calculated with PBE + vdW$^{\text{surf}}$.

| -0.74		-0.44		-0.29		-0.15		0		+0.15		+0.44		+0.74	
ini	TS	ini	TS	ini	TS	ini	TS	ini	TS	ini	TS	ini	TS	ini	TS
30.0	-99.3	27.0	-90.4	29.9	-79.4	24.7	-83.5	13.9	-80.0	-2.9	-77.1	-5.2	-70.0	-5.3	-56.0
35.5	115.2	31.6	121.0	71.1	118.8	76.0	119.3	75.3	117.7	70.5	114.4	59.4	107.4	63.8	96.8
106.2	167.5	103.2	180.4	115.9	183.8	107.7	180.5	97.9	183.4	78.5	186.2	60.5	183.4	70.8	170.1
125.2	309.2	131.4	369.1	129.9	386.8	158.8	389.4	172.9	393.5	189.9	402.6	202.2	413.5	205.6	414.1
262.6	356.7	196.9	396.4	416.1	413.6	437.9	417.0	449.2	429.3	457.8	434.5	409.4	449.3	378.0	457.4
309.4	602.6	219.3	645.5	470.6	643.6	478.8	642.9	473.6	646.7	463.4	653.7	462.2	673.3	468.0	722.8
1611.5	725.5	1593.7	736.9	1569.2	727.2	1569.1	732.9	1573.1	737.0	1576.4	761.1	1582.1	747.4	1592.0	751.1
3597.5	791.1	3604.3	774.4	3561.5	773.8	3579.4	774.6	3600.5	773.9	3618.5	783.0	3652.5	768.1	3665.8	832.4
3662.4	3605.4	3683.3	3620.3	3655.4	3624.1	3676.2	3626.5	3700.3	3628.5	3721.5	3634.5	3760.0	3632.9	3769.8	3623.6
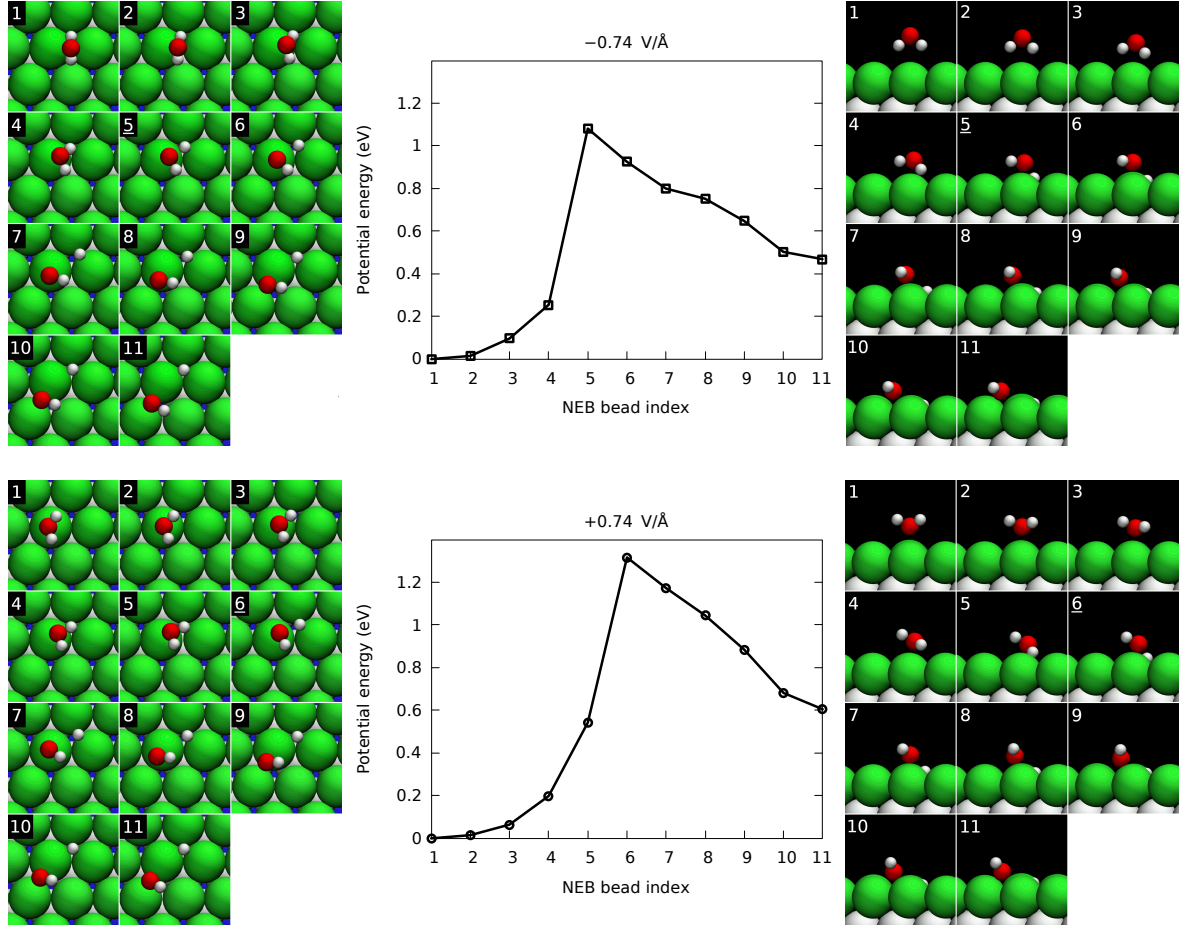
FIG. S1. Reaction path of water molecule splitting on the Pd(111) surface at –0.74 V/Å (top panel) and +0.74 V/Å (bottom panel), individual NEB beads and corresponding potential energies. Large green and white spheres denote the 1st and the 2nd layers of the Pd(111) surface, respectively. Blue spheres of the 3rd Pd layer are visible in the FCC hollow sites in the left-hand panels. The underlined frame index denotes the transition state.

III. TUNNELING UNDER THE DISSOCIATION BARRIER

We estimate tunneling crossover temperature as $T_c = \hbar\omega^{\mathrm{TS}}/(2\pi k_B)$, where ω^{TS} is the imaginary frequency of the unstable mode at the transition state. The results are given in Table S2. Thus, the role of tunneling in this reaction is negligible at relevant temperatures.
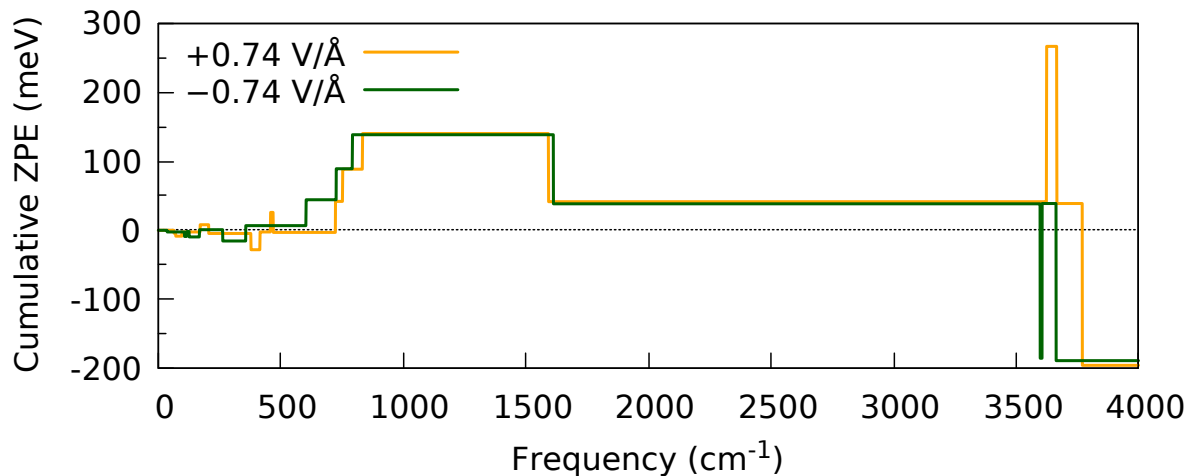
FIG. S2. Cumulative contribution of the vibrational modes to the total ZPE effect on the barrier of water dissociation, calculated by formula 1.

TABLE S2. Imaginary frequency of the unstable mode at the transition state (ω^{TS}) and the tunneling crossover temperature (T_c) for water dissociation on Pd(111) surface in different electric fields.

Electric field (V/Å)	ω^{TS} ($i * \text{cm}^{-1}$)	T_c (K)
+0.74	56.0	12.8
+0.44	70.0	16.0
+0.15	77.1	17.7
0	80.0	18.3
−0.15	83.5	19.1
−0.29	79.4	18.2
−0.44	90.4	20.7
−0.74	99.3	22.7

4